NO_x AND SO_2 ADSORPTION ON CARBON

Aurora M. Rubel and John M. Stencel
Center for Applied Energy Research
University of Kentucky
Lexington, KY 40511-8433, USA

Keywords: NO_x, SO_2, adsorption, carbon

INTRODUCTION

The need to control NO_x emissions from fossil fuel power plants has lead to the development of commercially proven technologies, the best known being selective catalytic reduction (SCR)[1-3]. Because NO_x concentrations are generally at near trace levels and less than 0.3%[4], a number of other potentially more efficient control measures have and are being investigated. One such measure includes the use of adsorbents such as metal oxides[5,6], ion-exchanged zeolites[7], activated carbon fibers with and without modifiers[8-10], and activated carbons[11-15].

Activated carbons can be used effectively for SCR and for the oxidation of SO_2 to SO_3 with the subsequent formation of H_2SO_4[16-19]. The uptake of SO_2 by carbons in the absence of NO_x has been studied extensively[20-26]. Moisture[20-22], O_2 content[22-25], and temperature[24] influence greatly the amount of SO_2 adsorbed onto activated carbons, although agreement is lacking on the synergistic or detrimental effects of co-adsorbed O_2 and H_2O[22-25]. It has been suggested that two different sites on the carbon are involved in SO_2 adsorption and oxidation[26], and that two different SO_2 species are present on the carbon during and after adsorption[22-25].

NO adsorption onto activated carbons over a temperature range of 20-120°C and in the absence of SO_2 have been reported[11-15, 27-29]. Without O_2, a carbon's NO uptake capacities and adsorption kinetics were low[27, 28] in comparison to when O_2 was present as a co-adsorbate[11-13]. These data have shown that the adsorption of NO from a simulated flue gas containing O_2, CO_2, and H_2O involved the catalytic conversion of $NO + \frac{1}{2} O_2 \rightarrow NO_2$ at active site(s) on the carbon[11-13] leading to NO_x adsorption capacities as high as 200 mg NO_2 (g carbon)$^{-1}$. No published work has been found which details adsorption capacities and kinetics during the co-adsorption of NO and SO_2 over activated carbons or other porous materials. However, an understanding of the effects of such co-adsorption is very important because the combustion flue gas from every type of fossil fuel will contain SO_2 and NO_x. Hence, this work was performed to elucidate interactions between NO_x and SO_2 in and over activated carbons during adsorption and desorption cycling.

EXPERIMENTAL

Instrumentation. NO_x/SO_2 adsorption/desorption profiles were obtained using a Seiko TG/DTA 320 coupled to a VG Micromass PC quadrupole mass spectrometer (MS). A heated (170°C) fused silica capillary was used to transfer an aliquot of the atmosphere above the sample pan in the thermogravimetric analyzer (TG) to an inert metrasil molecular leak which interfaced the capillary with the enclosed ion source of the MS. Both instruments were controlled by computers which also provided for programmable control of the furnace, continuous weight measurements, sweep gas valve switching, data acquisition and analysis, review of MS scans and export of data to other computers. The MS has a Nier type enclosed ion source, a triple mass filter, and two detectors (a Faraday cup and a secondary emissions multiplier).

TG-MS procedures. The TG sample pan was loaded with a constant activated carbon volume weighing approximately 20-30 mg. The sweep gas flow rate through the TG was held constant at 200 ml m^{-1} metered at room temperature and pressure. The heating regime of the furnace incorporated segments in the following order for pre-conditioning, cooling, adsorption, reversible desorption, and temperature-induced (irreversible) desorption. Explanations of each step and example programs have been previously published[11,13]. For this study, the pre-conditioning and irreversible desorption heating rate, adsorption time interval, reversible desorption time, and the maximum desorption temperature were 20 °C m^{-1}, 60 m, 30 m, and 350 ° C respectively. A He gas sweep was used during pre-conditioning, and reversible and irreversible desorptions. Pre-conditioned carbon was exposed to simulated flue gas only during the adsorption step. Multiple and consecutive adsorption/desorption cycles could be performed by recycling the furnace temperature program.

The MS was used to continuously monitor gases during an experiment. Spectral scans were acquired over a 1-100 a.m.u. range with a total measurement interval of approximately 30 s per 100 a.m.u..

Mass ion identification, analytical procedures, and materials. The identification of desorbed gases detected by the MS was done by using the major mass ions, 64, 44, 32, and 18, for SO_2, CO_2, O_2, and

H_2O respectively. The major mass ion for both NO and NO_2 is 30. The relative abundance of a.m.u. 46 for NO_2 gas is approximately 40 percent, but in mixtures of gases, this value can change. Therefore, NO and NO_2 were identified by comparing the mass ion ratio, 30/46, during desorption with ratios determined using mixtures of NO or NO_2 and all combinations of gases used during our study.

A carbon, commercially produced by physical activation with steam, was used. The carbon had N_2 BET total, meso- and micropore surface areas and pore volumes of 460, 20, and 440 $m^2\ g^{-1}$ and 0.69, 0.45, and 0.24 ml g^{-1} respectively. The chemical and physical properties of this carbon, identified as carbon, **a**, in a previous publication, has been described in detail[15]. Carbon pre-conditioned under a flow of He or SO_2 was used.

Three simulated flue gas mixtures were used during this study. The concentrations of O_2, CO_2, and H_2O were held constant at 5%, 15%, and 0.4-0.6% respectively. The NO and SO_2 composition of the three mixtures were varied as follows: 1% NO with 0% SO_2, 1% NO with 0.025% SO_2, and 0% NO with 0.025% SO_2. He was used as the balance gas. The primary variable studied was the simulated flue gas composition at an adsorption temperature of 70°C.

RESULTS AND DISCUSSION

Adsorption/desorption profiles shown in Figure 1 were generated during each TG/MS experiment. The weight gained, weight lost and an identification of the desorbed gas species were determined using these profiles. Figure 1 shows a profile for the co-adsorption of NO_2 and SO_2 at 70°C. Carbon pre-conditioning is performed up to point **a**. The weight gained upon exposure of the carbon to the simulated flue gas (points **a**-to-**b**) was attributed to the adsorption of gas components. Weight lost at the adsorption temperature after switching from the simulated flue gas to He (points **b**-to-**c**) was attributed to "reversibly adsorbed" species. Weight lost as a consequence of increasing the temperature of the carbon (points **c**-to-**d**, and beyond), i.e. during temperature programmed desorption (TPD), was attributed to two "irreversibly adsorbed" species which evolved at different temperatures. They were identified by MS as NO_2 and SO_2 and were the only evolved gas species detected. Upon reaching the maximum desorption temperature, the carbon weight returned to the pre-adsorption starting weight.

Weight gain curves during exposure of the activated carbon to the three different flue gas mixtures are presented in Figure 2. The total uptake decreased from 143 mg (g carbon)$^{-1}$ -to- 129 mg (g carbon)$^{-1}$ when SO_2 was a constituent in the gas. Pre-saturating the carbon with SO_2 prior to exposure to gases containing both NO and SO_2 decreased further the total uptake to 109 mg (g carbon)$^{-1}$. In the presence of SO_2 only (no NO), the uptake was only 24 mg (g carbon)$^{-1}$.

The desorption weight loss curves, presented in Figure 3, were defined with respect to reversible and irreversible (TPD) components. Reversible desorption accounted for 18%, 36% and 58% of the total uptake for gases containing both NO and SO_2, NO alone, or SO_2 alone, respectively. Figure 4 shows the DTG curves acquired during TPD and Figure 5 gives the desorption weights which could be attributed to specific evolved gases by MS. For simulated flue gas containing NO and SO_2, two irreversibly adsorbed species desorbed from the carbon and were identified to be NO_2 and SO_2. The temperature of maximum evolution was 145°C for NO_2 and 319°C for SO_2 (also see Figure 1). The adsorption of NO_2 in the absence of SO_2 also gave two irreversibly adsorbed species, having temperatures of maximum evolution at 144°C and 352°C. These two irreversible components were identified as NO_2 and CO_2, respectively. Only one irreversibly adsorbed species, identified as SO_2, was desorbed from the carbon after exposure to gas containing SO_2 (no NO). The maximum evolution of this SO_2 occurred at 302°C.

When SO_2 was present, the amount of irreversibly adsorbed NO_2 decreased to 68 mg (g carbon)$^{-1}$ from 87 mg(g carbon)$^{-1}$ when SO_2 was not present (Figure 5). The amount of irreversible NO_2 species further decreased to 59 mg (g carbon)$^{-1}$ when the carbon was pre-saturated with SO_2. However, the amount of irreversibly bound SO_2 was doubled when SO_2 was adsorbed in the presence of NO in comparison to when SO_2 was adsorbed by itself. This enhancement suggests that there is synergistic interaction between NO_2 and SO_2 during adsorption onto the carbon. Another observation was the fact that carbon pre-saturated with SO_2 and then exposed to the NO + SO_2 - containing flue gas (compare Figures 2 and 5) adsorbed more SO_2 than without the pre-saturation. Additionally, the temperature of desorption for the irreversibly adsorbed SO_2 species was increased from 300°C (in the case of SO_2 adsorption without NO) to 320°C when SO_2 and NO_2 are co-desorbed.

We have previously postulated that NO_2 adsorption involved the catalytic conversion of NO + ½ O_2 → NO_2 at an active site(s) on the carbon and that NO_2 then condenses within the micropores of the carbon[13]. It is possible that active sites are created during the co-adsorption of NO_2 and SO_2 that are

not created during the adsorption of SO_2 by itself, or the presence of NO_2 on the surface may assist the oxidation of $SO_2 \rightarrow SO_3$ on the carbon which enhanced the uptake of SO_2. Relative to the effects of SO_2 on the uptake capacity of NO_2 , it may bind to or interfere with the sites involved in the catalytic conversion of NO-to-NO_2, thereby resulting in lower NO_2 adsorption.

The temperature of maximum evolution of NO_2 was not altered by the presence of SO_2, indicating that the mechanism of condensation of NO_2 within the micropores was not affected by SO_2 surface species. Because condensation of NO_2 within the micropores would be strongly dependent on van der Waal forces[5,10,12], and because SO_2 and NO_2 have similar van der Waal force constants, it is possible that adsorbed SO_2 would not affect the NO_2 storage mechanism. However, SO_2 has a critical volume 1.5 times that of NO_2 and has stronger bonding to the carbon. Both of these factors would suggest that the adsorbed SO_2 species may concentrate at pore mouths, a location which would limit NO_2 condensation. The slower rate of reversible desorption when $NO_2 + SO_2$ are co-adsorbed (Figure 3) in comparison to adsorption of NO_2 alone may also reflect a physical impediment related to SO_2; for instance SO_2 bound to active sites could limit or block the access of NO_2 to the micropores, thereby affecting not only the storage capacity but also the rate of adsorption/desorption.

In fact, the maximum adsorption rate and the desorption rate for the irreversibly adsorbed NO_2 species were decreased by the co-adsorption of SO_2 (Figure 6). Good correlations ($r^2 = 1.00$) were obtained for the decline in the maximum adsorption rate (second order) and desorption rate (first order) versus the amount of SO_2 adsorbed. We have previously reported that the NO_2 adsorption capacity of different carbons was dependent on the maximum adsorption rate of NO_2, but that the desorption rate of the irreversibly adsorbed NO_2 species was the same for all carbons[15]. For the current study, the amount of NO_2 stored in the carbon versus the maximum adsorption rate, as influenced by SO_2, resulted in a good second order correlation, $r^2 = 0.995$ (Figure 7).

SUMMARY AND CONCLUSION

During the co-adsorption of NO_2 and SO_2 from a simulated flue gas, less NO_2 and substantially more SO_2 was adsorbed in comparison to when either oxide was adsorbed by itself. The adsorption mechanism for NO_2 remained unchanged in the presence or absence of SO_2. When NO_2 and SO_2 were co-adsorbed, a synergism improved the capacity of the carbon for SO_2 uptake. The presence of adsorbed SO_2 in the carbon significantly decreased the rate of adsorption and the rates of both reversible and irreversible desorption of NO_2, indicating the possibility of a physical impediment created by the adsorbed SO_2.

REFERENCES

1. Bosch, H. and Janssen, F. *Catal. Today* 1988, **2**, 369
2. Grzybek, T. and Papp, H. *Appl. Catal. B. Environ.* 1992, **1**, 271
3. Radtke, F., Koeppel, R.A., and Baiker, A. *Appl. Catal.* A 1994, **107**, L125
4. Ritter, J.A. and Yang, R.T. *Ind. Eng. Chem. Res.* 1990, **29**, 1023
5. Arai H. and Machida M., *Catalysis Today* 1994, **22**, 97
6. Stiles, A. B., Klein, M.T., Gauthier, P., Schwarz, S., and Wang, J. *Ind. Eng. Chem. Res.* 1994 **33**, 2260
7. Zhang, W.,Yahiro,H., Mizuno, N., Izumi, J., and Iwamoto, M., *Langmuir* 1993, **9**, 2337
8. Kaneko, K., Shindo, N. Carbon 1989, **27**, 815
9. Knoblauch, K., Richter, E. and Juntgen, H. *Fuel* 1981, **60**, 832
10. Kaneko, K., Nakahigashi, Y. and Nagata, K. *Carbon* 1988, **26**, 327
11. Rubel, A.M., Stencel, J.M., and Ahmed, S.N. *Preprints Symposium on Flue Gas Cleanup Processes* 1993, ACS, Division of Fuel Chem., Denver, CO meeting, 726.
12. Rubel, A.M., Stencel, J.M., and Ahmed, S.N. *Proceeding of the AIChE 1993 Summer National Meeting* 1993, Seattle, WA,, paper no. 77b.
13. Rubel, A.M., Stewart, M.L. and Stencel, J.M. *JMR* 1994, **10**, 562.
14. Rubel, A.M. and Stencel, J.M. *Energy and Fuel*, in press
15. Rubel, A.M., Stewart M.L., and Stencel, J.M. In *Reduction of Nitrogen Oxide Emissions, ACS Symposium Series 587*, Ozkan, U.S., Agarwal, S.K., and Marcelin, G. eds., ACS, Washington, D.C. 1995,208
16. Cha, C.Y. *Res. Chem. Imtermed.* 1994, **20**, 13
17. Gangwal, S.K., Howe, G.B., Spivey, J.J., Silveston, P.L., Hudgins, R.R., and Metzinger, J.G. *Environ. Prog.* 1993, **12**, 128
18. Ahmed, S.N., Stencel, J.M., Derbyshire, F.J., Baldwin, R.M. *Fuel Proc. Tech.* 1993, **34**, 123
19. Ahmed, S.N., Baldwin, R.M., Derbyshire, F.J., McEnaney, B., and Stencel, J.M. *Fuel* 1993, **72**, 287
20. Zawadzki, J. *Carbon* 1987, **25**, 43
21. Zawadzki, J. *Carbon* 1987, **25**, 495
22. Tartarelli, R., Davini, P., Morelli, F., and Corsi, P. *Atmosph. Environ.* 1978, **12**, 289

23. Davini, P. *Carbon* 1991, **28**, 565
24. Davini, P. *Carbon* 1991, **29**, 321
25. Carrasco-Marin, F., Uterra-Hidalgo, E., Rivera-Utrilla, J., Moreno-Castilla, C. *Fuel*, 1992, **71**, 575
26. Mochida, I., Hirayama, T., Kisamori, S., Kawano, S., and Fujitsu, H. *Langmuir* 1992, **8**, 2290
27. Teng, H. And Suuberg, E.M. *J. Phys. Chem.* 1993, **97**,478
28. DeGroot, W.F., T.H. Osterheld, G.N. Richards. *Carbon* 1991, **29**,185
29. Richter, E., R. Kleinschmidt, E. Pilarczyk, K. Knoblauch, and H. Juntgen. *Thermochimica Acta* 1985, **85**,311

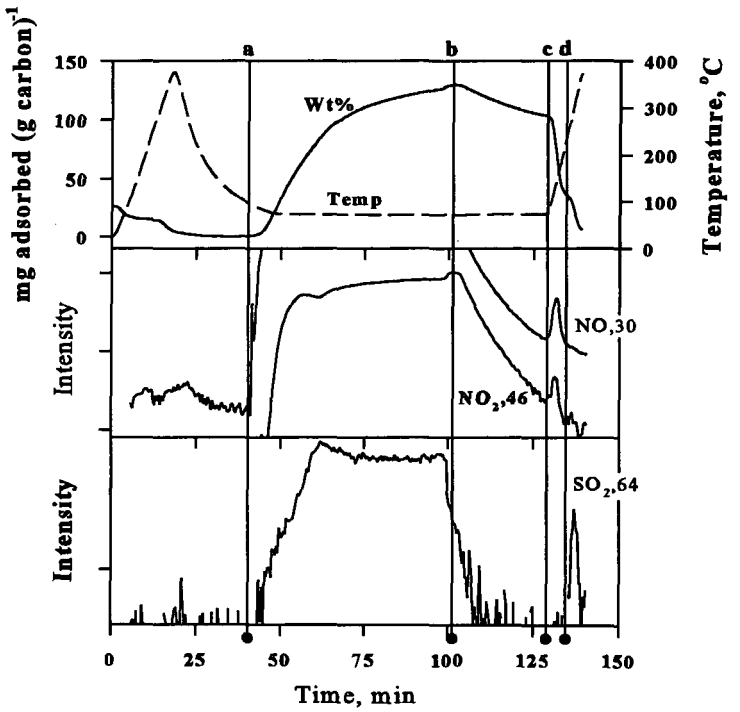

Figure 1. Adsorption-desorption profile from TG-MS for adsorption of NO_2 and SO_2 at 70°C.

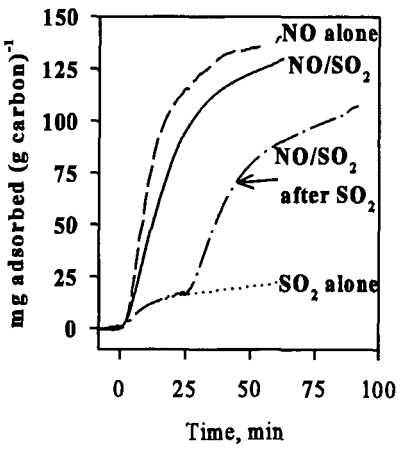

Figure 2. Weight gain curves during adsorption.

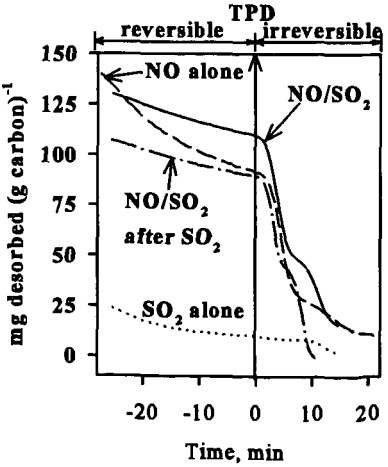

Figure 3. Weight loss curves during TPD.

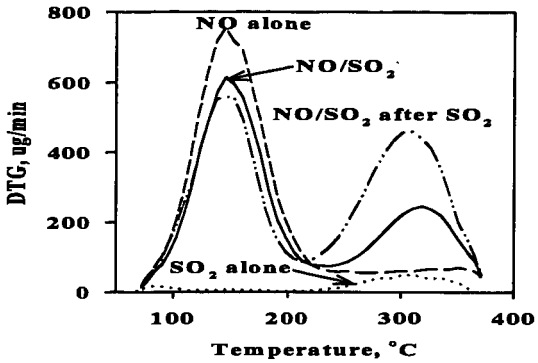

Figure 4. DTG curves during irreversible desorption.

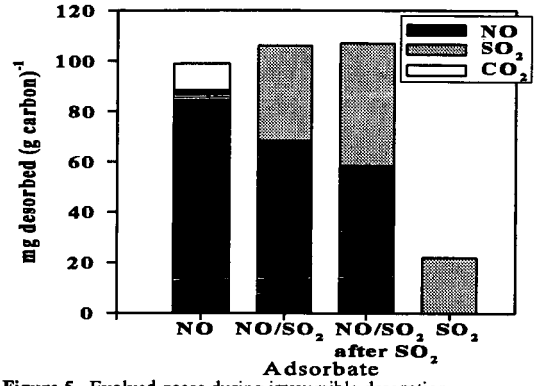

Figure 5. Evolved gases during irreversible desorption.

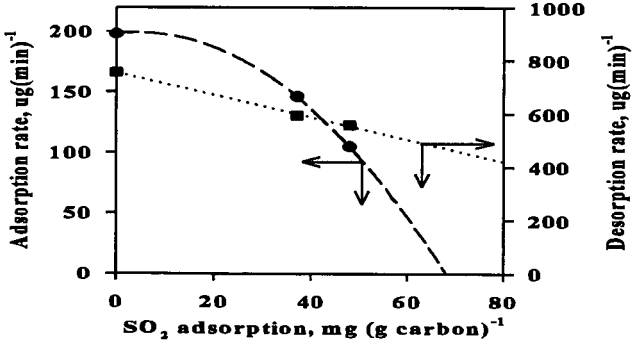

Figure 6. Influence of adsorbed SO_2 on adsorption and desorption rates.

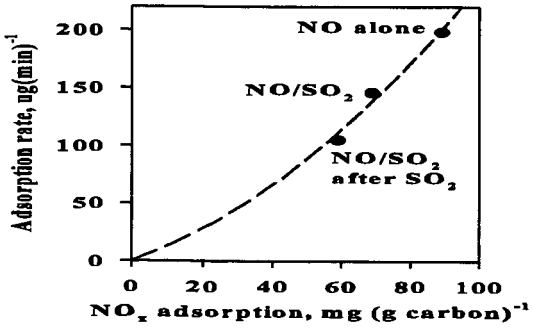

Figure 7. Correlation between NO_x adsorption capacity and total adsorption rate.